J Appl Electrochem (2012) 42:989–995
DOI 10.1007/s10800-012-0442-0

SHORT COMMUNICATION

Investigation on $Li_4Ti_5O_{12}$ batteries developed for hybrid electric vehicle

Kai Wu · Jun Yang · Yao Zhang · Chenyun Wang · Deyu Wang

Received: 8 April 2012 / Accepted: 19 June 2012 / Published online: 8 July 2012

Abstract Carbon-coated nano-$Li_4Ti_5O_{12}$ (LTO) anode material was prepared and evaluated with 5.5 Ah pouch cells, paired with $LiNi_{1/3}Co_{1/3}Mn_{1/3}O_2$ cathode for potential hybrid electric vehicle (HEV) application. The as-prepared LTO batteries showed excellent electrochemical performance. They delivered a peak discharge power density of ca. 2,800 W kg^{-1}, and featured a high power (94 and 92 % of discharge and charge capacity at 20 C, respectively) and a prolonged cycle life (89 % capacity retention after 5,000 cycles at 10 C charge and discharge rate). However, the severe capacity decay was observed at elevated temperatures because of loose (worse) interfaces caused by gas generation. It was found that H_2 was the dominant gas component, and the inflation rate had an Arrhenius-type correlation with storage temperature. The battery inflation, arising from side reactions between electrolyte and LTO anode, is the major technical barrier for practical application of the LTO batteries in HEV.

K. Wu · J. Yang (✉)
School of Chemistry and Chemical Engineering, Shanghai Jiao Tong University, 800 Dongchuan Road, Shanghai 200240, People's Republic of China
e-mail: yangj723@sjtu.edu.cn

K. Wu · Y. Zhang
Amperex Technology Limited, 1 West Industrial Road, North Zone of SSL Sci.&Tech. Industry Park, Dongguan 523808, People's Republic of China

C. Wang · D. Wang (✉)
Ningbo Institute of Material Technology and Engineering, Chinese Academy of Science, 519 Zhuangshi Road, Ningbo 315201, People's Republic of China
e-mail: wangdy@nimte.ac.cn

Keywords: Lithium ion battery · $Li_4Ti_5O_{12}$ anode · Battery inflation · Hybrid electric vehicle

1 Introduction

Lithium ions can be electrochemically intercalated into/de-intercalated from spinel lithium titanate ($Li_4Ti_5O_{12}$, LTO) with a theoretical capacity of 175 mAh g^{-1} in the voltage range of 1.0–2.5 V versus Li^+/Li [1]. LTO belongs to the group of the so-called "zero-strain" insertion material (no change in lattice parameters during intercalation) and is regarded as an ideal candidate for long-life lithium ion batteries [2, 3]. The LTO-based lithium ion battery is intrinsically safer than the graphite-based one because the reaction of the fully lithiated LTO anode with electrolyte releases much less heat [4]. Rate capability of LTO can be better compared with graphite and other amorphous carbon, because of the lower de-solvation energy of Li^+–solvent complex [5] and no SEI formation on its surface. Moreover, lithium dendrite hardly forms even if charged at high C-rate and/or at low temperature owing to LTO's relatively high redox potential (1.55 V vs. Li^+/Li). This further benefits its safety and long life characteristics.

Extensive efforts in battery R&D community have been focused on improving the performance of LTO-based cells. It has been demonstrated that rate capability of LTO can be significantly enhanced by grain/particle size reduction [6–8], doping [9–11], and forming composite with carbon or other conducting materials [12, 13]. Tap density of LTO powder can be raised by particle morphology control [14]. In addition, energy density of LTO-based lithium ion battery can be increased without compromising cycle life and rate capability via the choice of the high-voltage and high-

capacity spinel Li[$Ni_{0.45}Co_{0.1}Mn_{1.45}$]$O_4$ cathode material [15]. Therefore, the LTO-based lithium ion battery has been considered as one of the most promising candidates for energy storage systems such as HEV and electric grid (for peak shaving) [16–18], which require a high power-to-energy ratio, proven safety, and prolonged cycle life. In this study, 5.5 Ah pouch cells, composed of carbon-coated nano-LTO anode and $LiNi_{1/3}Co_{1/3}Mn_{1/3}O_2$ (NMC) cathode, were prepared and evaluated. The as-prepared LTO battery showed excellent rate capability and cycle life at ambient temperature. However, the battery inflated when stored or cycled at high temperature, which poses a major technical barrier for future commercialization. To our knowledge, this phenomenon has not been formally reported in the academic literature so far, and therefore neither has it received enough attention by the battery R&D community. The underlying reason is that coin cells have been used for most studies, in which inflation can hardly be observed. In this article, the performance of the large format pouch-type LTO battery developed for HEV application is reported with the emphasis on our findings of the inflation. The mechanism behind this phenomenon and its correlation with store temperature are discussed herein.

2 Experiments

2.1 $Li_4Ti_5O_{12}$ material

Spinel $Li_4Ti_5O_{12}$ was prepared by a solid-state synthetic route. Stoichiometric amounts of Li_2CO_3 (Chinese Lithium Com., 99.9 %) and TiO_2 (Pule Chem., 99 %) were ball-milled with appropriate amounts of sugar for 4 h and sintered at 800 °C for 24 h under N_2. After being cooled down to room temperature, the powder was pulverized and vacuumed in Al-plastic laminate foil for storage.

LTO electrodes for coin cell evaluation were fabricated by casting the slurries containing 90 wt% $Li_4Ti_5O_{12}$, 5 wt% Super P, and 5 wt % poly(vinylidene fluoride) (PVdF) (HSV 900, Kynar) in *N*-methyl-pyrollidone (NMP) on Al-foil. After drying at 100 °C under vacuum, the electrode was calendared to 1.7 g cm^{-3}, and then punched into ϕ 1.4-cm-diameter disks with an average active material loading of 10 mg cm^{-2}. The electrode disks were subsequently assembled into 2032 coin cells using Li metal foil as the counter electrode, Celgard® 2500 as separator, and 1 mol $LiPF_6$ in ethylene carbonate (EC), dimethyl carbonate (DMC), and ethyl methyl carbonate (EMC) (1:1:1, w/w) as the electrolyte. The test cells were assembled in an M-Braun glove box filled with purified argon. The moisture and oxygen levels of the glove box were less than 1 ppm.

2.2 LTO batteries

Home-made $Li_4Ti_5O_{12}$/C was used as anode active material. $LiNi_{1/3}Co_{1/3}Mn_{1/3}O_2$ (NMC), natural graphite (NG), and the electrolyte were purchased from 3M (Shanghai, China), BTR (Shenzhen, China), and Shanshan (Dongguan, China), respectively. As-prepared 50J0A7-type (internal model) LTO batteries have a capacity of 5.5 Ah. Both LTO and NMC electrodes were composed of 90 wt% active materials, 5 % PVdF, and 5 wt% Super-P. The coating weight was controlled at 5.3 mg cm^{-2} for LTO electrode and 7.1 mg cm^{-2} for NMC. 1 mol/L $LiPF_6$ in EC, DMC, and EMC (1:1:1 in wt% ratio) was used as electrolyte, with Celgard® 2500 as separator.

For a comparison, 50J0A7-type graphite batteries were also assembled. Graphite electrode was made of 96 wt% graphite, 2 wt% PVdF, and 2 wt% Super P. The recipe of NMC electrode was the same as that of LTO batteries. The coating weights of graphite and NMC electrode were 4.9 and 10.2 mg cm^{-2}, respectively. The other materials and manufacturing processes were the same as LTO batteries.

2.3 Measurements

The coin cells with LTO and Li foil electrodes were evaluated in the voltage range from 1.0 to 2.5 V on a PC-controlled Land 2000 battery tester at 0.2 C. The specific capacity was calculated on the basis of the amount of active materials. 5.5 Ah pouch batteries were tested on a PC-controlled Arbin BT2,000-5V200A within a voltage range of 1.5–2.8 V and 3.0–4.2 V for LTO and graphite batteries, respectively. Power density of LTO battery was characterized by Hybrid Pulsed Power Characterization (HPPC) as defined in battery test manual for Plug-In hybrid electric vehicle (P5–P8, US DOE, 2008). The HPPC test was used to evaluate the 10-s discharge and the 10-s regeneration power capabilities at every 10 % depth-of-discharge (DOD) increment.

The baking experiments were carried out in a temperature-controlled oven. The as-prepared LTO batteries were kept at different temperatures. The thicknesses were measured at 6-h intervals for the batteries stored at 40, 50, 55, and 60 °C, and at 1-h intervals for the samples stored at 70, 80, and 85 °C. As the cell thickness increase reached 10 %, the test was terminated, and the samples were analyzed. To explore the origin of gases, the full-charged LTO batteries were disassembled in a dry room. The separated cathode and anode membranes were vacuum sealed in different bags and kept at 55 °C for 2 weeks. The graphite batteries were tested under the same condition as the control.

Powder XRD patterns were measured using a PANalytica X'Pert PRO SUPER (Cu Kα radiation, 2θ step size of 0.017). The morphology of LTO was observed with

scanning electron microscopy (JEOL6390). The carbon content was measured with elemental analyzer (PE2400II). gas-chromatography (GC) was conducted in a PC-controlled Agilent 7890A to analyze the gas compositions in batteries. Thermal analysis (TG–DSC) was performed with 10 °C min^{-1} as heating rate in argon atmosphere via a thermogravimetric–differential scanning calorimetry apparatus STA-449C (Netzsch, Germany). The LTO and graphite electrodes for DSC characterization were sampled from LTO and graphite batteries (100 %SOC) in an argon-filled glove box and were tested without any further treatment.

3 Results and discussion

Carbon-coated LTO material was synthesized via a solid-state route in lab. As shown in Fig. 1a, its XRD pattern can be indexed as a single spinel phase of $Li_4Ti_5O_{12}$ (space group: *Fd*3-*m*) without any reflection peaks from other impurity phases. The particle size was approximately 300 nm, as observed by SEM (Fig. 1b), and carbon content was 1.6 %, as determined by elemental analyzer. The as-prepared LTO material was first electrochemically evaluated in a coin cell. It delivered a reversible discharge capacity of 159 mAh g^{-1} at 0.2 C with a plateau at 1.55 V versus. Li^+/Li (Fig. 1c). Figure 1d presents the results obtained from the DSC analysis of lithiated $Li_4Ti_5O_{12}$ and graphite anodes. It can be found that the total heat released from lithiated LTO electrode was significantly smaller than that from graphite. Our test data on the as-prepared LTO were comparable to the previously reported results [4, 12, 13, 19, 20].

The 50J0A7-type LTO batteries with a capacity of 5.5 Ah were assembled to further evaluate electrochemical performance of the LTO anode material in practical batteries. Figure 2 shows the typical charge–discharge curve of LTO/$LiNi_{1/3}Co_{1/3}Mn_{1/3}O_2$ battery in voltage range of 1.5–2.8 V at 1 C. The cell delivered a capacity of 5.5 Ah with a columbic efficiency of 99.99 %. The average discharge voltage was 2.25 V. LTO batteries also exhibited a good rate capability (as shown in Fig. 3a, b) in both charge and discharge conditions. At 20 C, the LTO batteries delivered 92 % of charge capacity and 94 % of discharge capacity (against 1 C capacity), respectively. In other words, more than 90 % capacity could be charged and

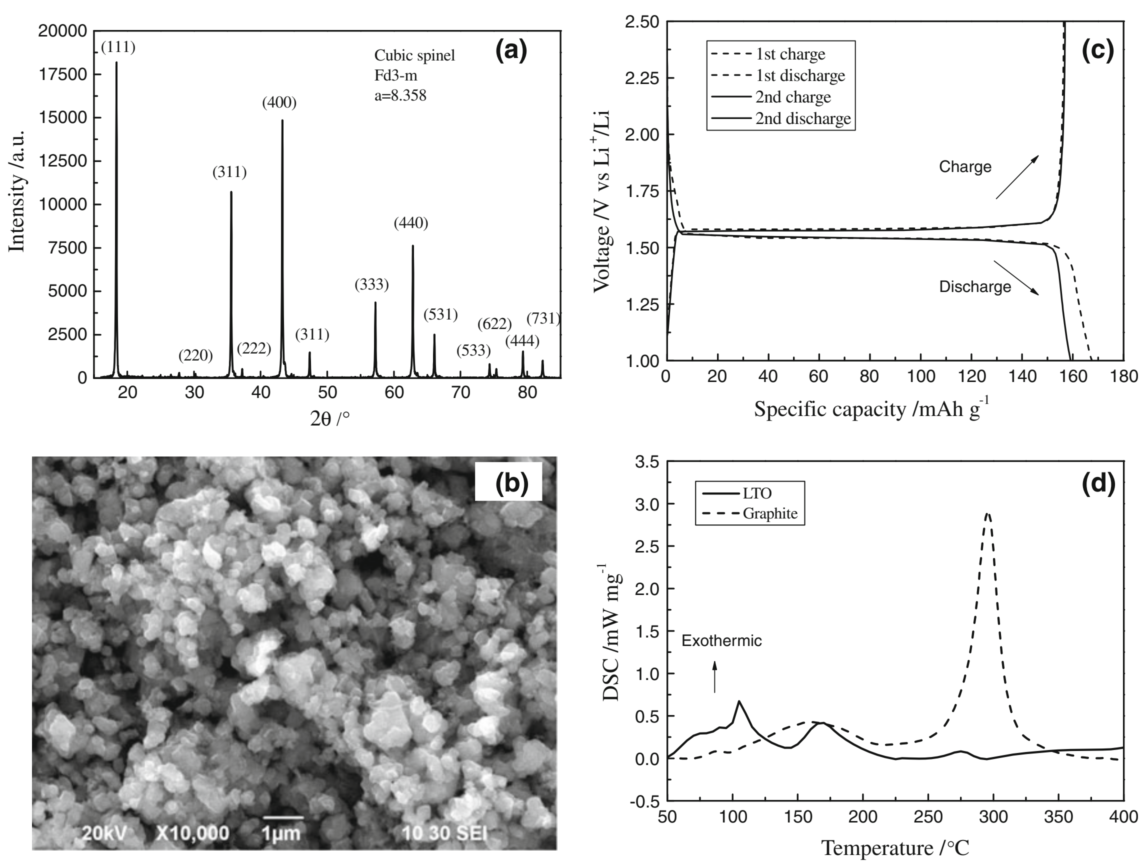

Fig. 1 Characterization of home-made $Li_4Ti_5O_{12}$/C: **a** XRD pattern; **b** SEM image; **C** charge–discharge curves of $Li_4Ti_5O_{12}$/C in coin cell; **d** DSC curves of lithiated LTO and graphite

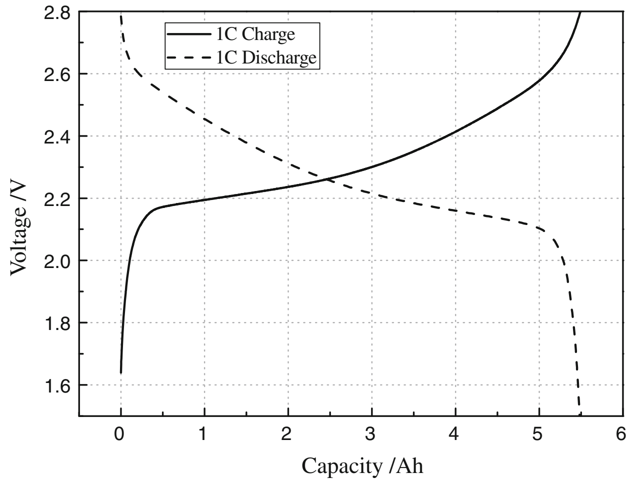

Fig. 2 Charge-discharge curves of 50J0A7-type LTO-NMC batteries at room temperature and 1 C rate. Voltage range: 1.5–2.8 V

discharged within 3 min. Furthermore, the HPPC power density at different depths of discharge was measured and compared in Fig. 3c. Both charge and discharge power densities were higher than 2000 W kg^{-1} within the range from 20 to 60 % DOD. In summary, the LTO batteries developed in our lab demonstrated satisfactory rate capability and power density for HEV application.

Cyclability is another critical characteristic for HEV batteries. Figure 4 shows the cycle performances of the home-made LTO and graphite cells at 25 and 55 °C, respectively. The LTO cells were cycled at a current rate of 10 C (55 A) and 100 % DOD, while the graphite cells were cycled at a rate of 0.5 C (2.75 A) and 100 % DOD. LTO cell demonstrated excellent cyclability at ambient temperature, and retained 89 % of the capacity after 5000 cycles. As the working temperature enhanced to 55 °C, the capacity faded to 80 % after only 720 cycles. By contrast, the graphite cells showed inferior performance. The capacity faded to 80 % after 1000 cycles at 25 °C, and after 550 cycles at 55 °C. It is known that graphite experiences a volume change of approximately 10 % during intercalation, which occurs mostly at a potential of <0.3 V versus Li^+/Li. As a result, the notable capacity fade of graphite cell can be attributed to the following mechanisms: 1) Irreversible lithium ion loss by SEI formation, breakdown, and recovery; 2) Transition metal ion's dissolution from cathode and reduction on anode; and 3) Electrical contact loss of active graphite particles. On the contrary, LTO is a type of "zero-strain" anode material and operates at a relatively high potential (approximately 1.55 V vs Li^+/Li). Therefore, either irreversible lithium ion loss or electrical contact loss, associated with low operating voltage and volume change, could be avoided for LTO cells, and the superior cyclability was obtained.

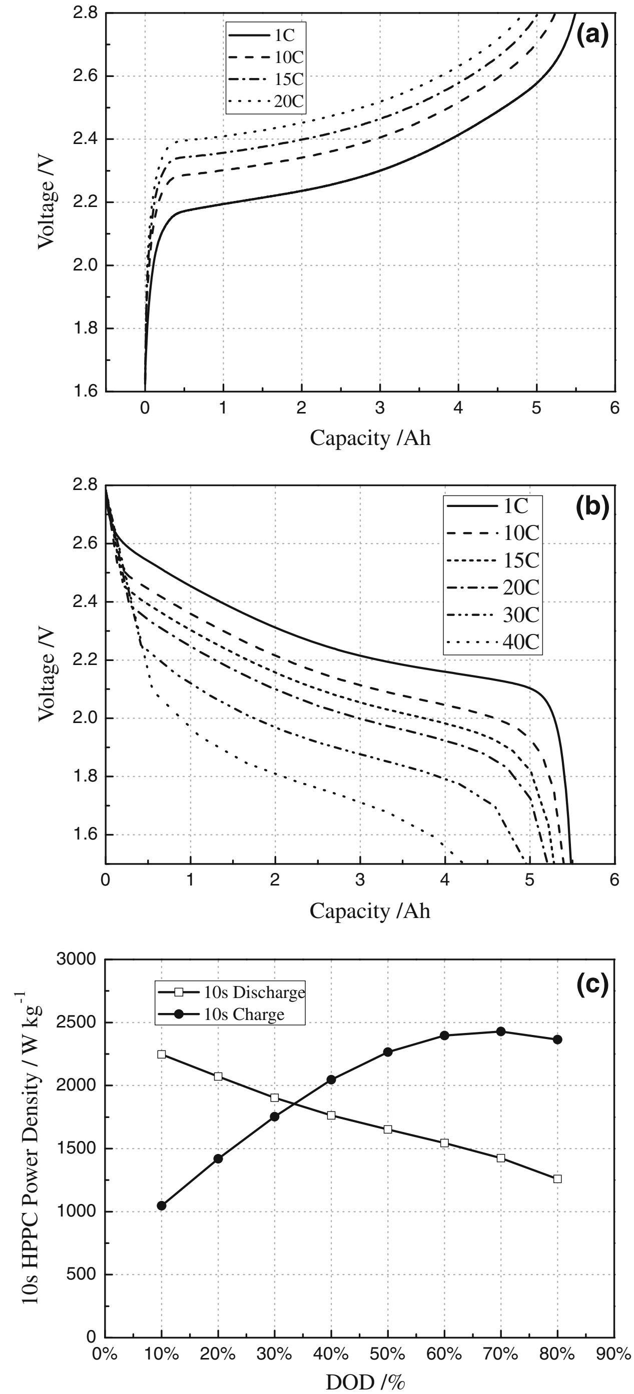

Fig. 3 Rate capability of 50J0A7-type LTO-NMC batteries at room temperature (voltage range: 1.5–2.8 V) **a** charge curves at various C rates, **b** discharge curves at various C rates, and **c** power density at different depth of discharge (DOD)

However, LTO cells are much more sensitive to working temperature as shown in Fig. 4. This unexpected cycle life degradation is ascribed to the cell inflation arising from gas release at high temperature (Fig. 5). Thickness increase of LTO cell was less than 1 % after 5,000 cycles at 25 °C, but

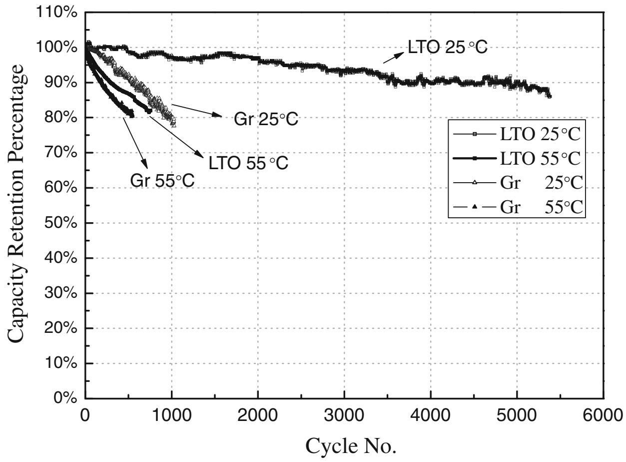

Fig. 4 Cycle life comparison of the LTO-NMC and Graphite-NMC batteries at 25 and 55 °C

it reached 18 % after 720 cycles at 55 °C. During gas evolution, not only the solvents of electrolyte can be consumed, but also the ionic and electronic transfer channels can be blocked, resulting in a high polarization for the electrochemical reaction. Usually, gas evolution in cells is related to some side reaction between electrolyte and electrodes. To investigate the origin of gas generation, the fully charged LTO–NMC batteries were disassembled in a dry room. Then, vacuum-sealed cathode and anode samples were baked at 55 °C for 2 weeks. The graphite–NMC batteries were tested at the same condition for a comparison. As shown in Fig. 6, the thickness of pouch bag containing graphite and NMC electrodes increased only 0.2 % afterward, whereas the thickness of the LTO bag increased by as high as 82 %. GC analysis results of the gas species in the stored LTO anode alone, cycled, and stored full cells are compared in Table 1. The cycled and stored full cells show similar gas compositions and contents, suggesting that similar side reactions occurred on LTO anode surfaces during storage and cycling. Among the detectable gases, the dominant species was hydrogen constituting over 80

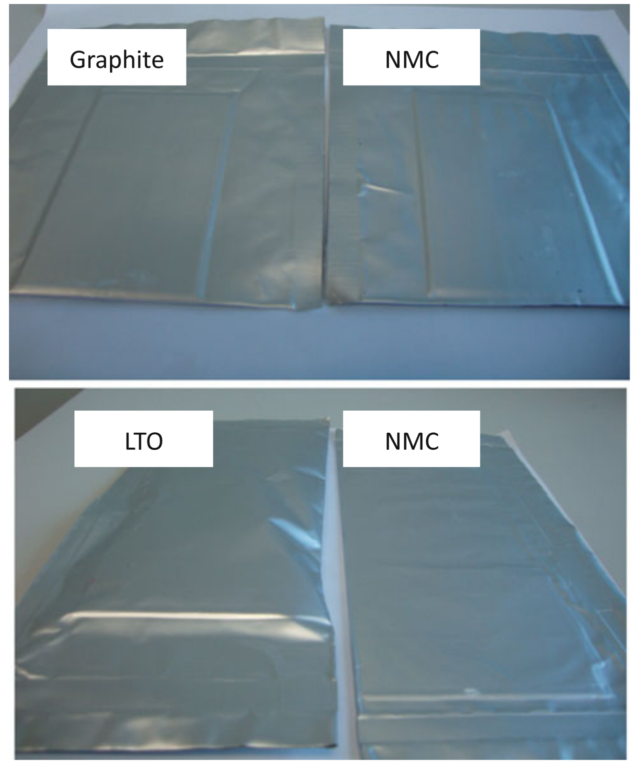

Fig. 6 Photos of LTO, NMC and graphite electrodes stored at 55 °C for 2 weeks

wt% in the mixture. The underlying mechanism needs to be further investigated.

To understand the influence of temperature on the inflation rate, the fully charged cells were baked at 40, 50, 55, 60, 70, 80, and 85 °C,. Gas analysis was carried out for the selected samples, and the results are shown in Table 2. For all the tested batteries, the gas species and compositions were quite similar, indicating that the existing test temperatures had little influence on the types of side reactions. Moreover, a specific parameter—"time to fail" (TTF)—is defined as the time to reach 10 % cell thickness increase, since the baking experiments were terminated

Fig. 5 Photos of the LTO battery before and after *cycling* at 55 °C

Table 1 Gas species and composition (wt%) of batteries cycled and stored at 55 °C

Sample	CO_2	C_2H_4	C_2H_6	C_3H_6	C_3H_8	H_2	CH_4	CO
Cycled full cell	2.47	2.45	0.49	0.01	0.00	86.38	2.52	5.68
Stored Full cell	1.42	2.56	0.65	0.00	0.05	86.63	3.50	5.19
Stored LTO anode	3.82	0.51	0.08	0.04	0.00	94.76	0.17	0.61

Table 2 Gas composition (wt%) of LTO cells stored at different temperature

Temperature(°C)	CO_2	C_2H_4	C_2H_6	C_3H_6	C_3H_8	H_2	CH_4	CO
40	1.42	2.56	0.65	0.00	0.05	86.63	3.50	5.19
55	1.42	2.56	0.65	0.00	0.05	86.63	3.50	5.19
70	1.29	1.49	0.42	0.01	0.04	90.04	2.71	4.00
80	0.77	2.08	0.36	0.01	0.03	91.11	2.29	3.36

Table 3 Time to failure (TTF) of 5.5 Ah fully charged LTO batteries at various storage temperatures

Temperature (°C)	40	50	55	60	70	80	85
Time to fail (TTF, h)	1536	612	288	216	18	6	3

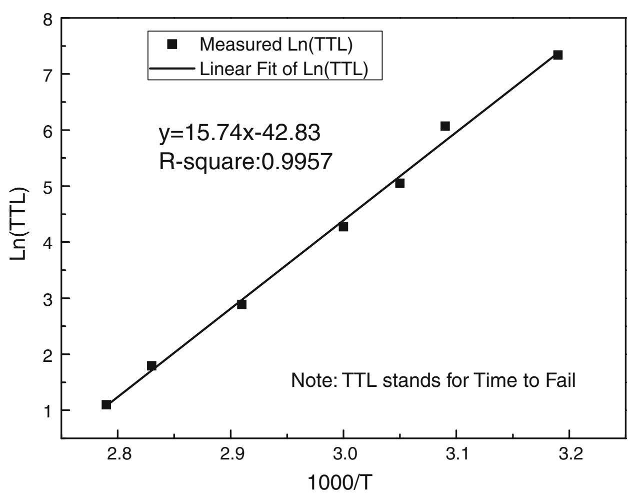

Fig. 7 Arrhenius fitting of time to failure (TTF) and storage temperature

afterward. Corresponding TTF values in this study are shown in Table 3 TTF numbers were shortened from 1536 h at 40 °C to 156 h at 55 °C, and to 6 h at 80 °C. It is clear that the inflation rate is strongly dependent on storage temperature.

During the data analytic process, we found that inflation rate ($v_{\text{inflation}}$) and working temperature roughly obeyed Arrhenius relation. The thickness variation in this case could be represented as Eqs.1 and 2:

$$\Delta h_{\text{thickness}} = v_{\text{inflation}} \times t = A \exp(-E_a/RT) \times t \tag{1}$$

$$\begin{aligned}\ln(\text{TTF}) &= E_{\text{a}}/\text{RT} + \ln(\Delta h_{\text{thickness}} \rightarrow 10\%) - \ln(A) \\ &= k/T + b\end{aligned} \tag{2}$$

where A and E_a are constants, and k and b are the slope and intercept, respectively of the fitting line when plotting ln(TTF) versus 1/T.

The TTF and temperature data are plotted in Fig. 7. Calculated from the fitting equation, it could be predicted that it will take ca. 6 years to swell by 10 % at 20 °C, and 1 year at 30 °C. This is far less than the calendar-life requirement of more than 15 years for HEV and grid applications.

It appears that LTO batteries cannot be applied in HEV before the inflation problem reported here is resolved. The improvements on LTO material, electrolyte, and battery design may suppress or even eliminate the battery inflation. Nevertheless, the current LTO battery could be used in some specific fields where super-long cyclic life is required, and the temperature can be closely monitored and controlled.

4 Conclusions

The home-made LTO battery exhibits an excellent electrochemical performance under limited temperature condition. It can fulfill the requirements of HEVs in term of power density and cycle life. However, the unexpected inflation problem, which is temperature sensitive, is hindering its commercialization. Gassing problem is most likely the last technical barrier for wide induction of LTO batteries in HEVs.

Acknowledgments The authors thank Amperex Technology Limited Co. (ATL) for the financial support. Dr. Deyu Wang and Mr. Chenyun Wang are indebted to Ningbo Key Innovation Team (grant no. 2011B82005), and gratefully acknowledge the start-up funding of the Ningbo Institute of Material Technology and Engineering, the Chinese Academy of Science.

References

1. Colbow KM, Dahn JR, Haering RR (1989) J Power Sources 26:397
2. Ozuku T, Aeda A (1994) Solid State Ionics 69:201
3. Ozuku T, Aeda A, Yamamoto N (1995) J Electrochem Soc 142:1431
4. Belharouak I, Sun YK, Lu W, Amine K (2007) J Electrochem Soc 154:A1083
5. Xu K, Cresce AV, Lee U (2010) Langmuair 26:11538
6. Wang D, Ding N, Song XH, Chen CH (2009) J Mater Sci 44:198
7. Lim J, Choi E, Mathew V, Kim D, Ahn D, Gim J, Kang S, Kim J (2011) J Electrochem Soc 158:A275
8. Prakash AS, Manikandan P, Ramesha K, Sathiya M, Tarascon JM, Shukla AK (2010) Chem Mater 22:2857
9. Yoshikawa D, Kadoma Y, Kim JM, Ui K, Kumagai N, Kitamura N, Idemoto Y (2010) Electrochim Acta 55:1872
10. Yi TF, Shu J, Zhu YR, Zhu XD, Zhu RS, Zhou AN (2010) J Power Sources 195:285
11. Cai R, Yuan T, Ran R, Liu XQ, Shao ZP (2011) J Energ Res 35:68
12. Xiang HF, Tian BB, Lian PC, Li Z, Wang HH (2011) J Alloys Compd 509:7205
13. Li X, Qu MZ, Huai YJ, Yu ZL (2010) Electrochim Acta 55:2978
14. Gao J, Jiang CY, Wan CR (2010) J Electrochem Soc 150:K39
15. Jung HG, Jang MW, Hassoun J, Sun YK, Scrosati B (2011) Nat Commun 2:516
16. Belharouak I, Koenig GM, Amine K (2011) J Power Sources 196:10344
17. Yi TF, Jiang LJ, Shu J, Yue CB, Zhu RS, Qiao HB (2010) J Phys Chem Sol 71:1236
18. Amine K, Belharouak I, Chen Z, Tran T, Yumoto H, Ota N, Myung ST, Sun YK (2010) Adv Mater 22:3052
19. Wu HC, Wu HC, Lee E, Wu NL (2010) Electrochem Commun 12:488
20. Jianga CH, Ichihara M, Honma I, Zhou HS (2007) Electrochim Acta 52:6470